

## A Novel PWM Inverter Switching Strategy for a Dual Two-level Inverter Fed Open - end Winding Induction Motor Drive

V.T.Somasekhar, K.Gopakumar SM IEEE, Andre Pittet SMIEEE, V.T.Ranganathan SM IEEE,

**Abstract**--A dual two-level inverter fed open-end winding induction motor drive is proposed in this paper. A total of 64 voltage space phasor combinations are possible in this scheme as each inverter produces eight voltage space phasors. The proposed scheme produces voltage space phasor locations similar to that of a 3-level inverter. In a 3-level Inverter the series connected DC link capacitors carry the load current. This results in a fluctuating voltage space phasors, which is undesirable. Also, a 3-level inverter requires a bulky DC link capacitor. In the proposed scheme the DC link capacitor carries only the ripple current and hence the voltage space phasor fluctuations are absent. A novel PWM switching strategy aimed to suppress the zero sequence currents is also proposed in this paper, without the need for harmonic filters and Isolation transformers.

**Index Term**- Open-end winding Induction motor, PWM technique

### I. Introduction

The dual two-level inverter fed open-end winding induction motor drives offer certain advantages compared to the three-level inverter drives such as - redundancy of the space vector combinations for the same number of space vector locations and the absence of neutral point fluctuations. The pioneering work on the dual inverter fed open-end winding induction motor drive was done by H.Stemmler and P.Guggenbach [3]. In this work, two two-level inverters connected at either end of the open-end winding induction motor, employing the sine-triangle PWM, have driven the motor. E.G.Shivakumar et al. have suggested a space-vector based PWM scheme for the dual-inverter driven open-end winding induction motor drive [7]. In this scheme [7], the common mode voltages (the harmonics of the triplen order) in the phase of the motor were suppressed by employing an isolated DC-power supply for each inverter. Thus, this scheme requires two isolation transformers for realizing two isolated DC-power supplies. In this paper, an alternative PWM scheme is suggested which is based on the space-vector modulation. This PWM scheme eliminates the need for the isolation transformers, thus saving a substantial cost. The proposed space vector PWM is based on voltage space-vector combinations in the dual inverter scheme that do not contribute to the triplen harmonics.

V.T.Somasekhar, K.Gopakumar, Andre Pittet are with CEDT, Indian Institute of Science, Bangalore-560012, INDIA.

E-mail - kgopa@cedt.iisc.ernet.in

V.T. Ranganathan is with EE dept, IISc.

### II. Dual inverter fed induction motor with open-end winding

The schematic of the dual voltage source inverter fed three-phase induction motor with open-end winding is shown in Fig. 1.  $V_{a0}$ ,  $V_{b0}$ ,  $V_{c0}$  are the pole voltages of the inverter-1.  $V_{a'0}$ ,  $V_{b'0}$ ,  $V_{c'0}$  are the pole voltages of inverter-2. The space phasor locations from individual inverters are shown in Fig.2. The space phasor combinations (64- combinations) from the two inverters are shown in Fig.3. For the primitive scheme shown in Fig.1, a significant triplen harmonic content is expected in the inverter phase currents, because of the lack of an isolated neutral point. Different space phasor combinations will have different third harmonic voltage magnitudes. This can be computed from the pole voltages due to various switching combinations from individual inverter [7]. For example, a combination 6-1' implies that the switching state for inverter-1 is (+ - +) and that for inverter-2 is (+ - -). A '+' indicates that a top switch in an inverter leg is turned on and a '-' indicates that the bottom switch in an inverter leg is turned on. The motor phase voltage can be found out from the pole voltages from individual inverters. Since the triplen harmonic voltages are in phase, the sum of the phase voltages not being equal to zero implies the presence of triplen harmonic content. The triplen harmonic contribution (relative magnitudes) from different space phasor combinations is shown in Table-1. There are twenty space phasor combinations whose third harmonic contribution is zero (Table-1) [7]. To avoid the triplen harmonic currents, the extreme space phasor locations used for the present work are shown in Fig.4. When these space phasor combinations are used, then the maximum magnitude of the fundamental gets reduced (Fig.4). However, by giving an additional boost to the DC-link voltage it is possible to obtain the rated phase voltage of the motor from the present dual inverter configuration. Because of the dual inverter configuration, the actual DC-link voltage to be applied across the DC-bus would be  $V_{dc}/2$  (where  $V_{dc}$  is the Conventional two - level inverter DC link Voltage). With a DC-link voltage of: 295Volts, a rated phase voltage (rms) of 230V, can be obtained in Six-step mode for the proposed scheme.

#### III. Dual inverter with auxiliary switches

The proposed power circuit schematic is shown in fig.5. The auxiliary switches SA<sub>1</sub> through SA<sub>4</sub> are bi-directional controlled switches. From Table-I, it may be observed that there are certain space phasor combinations that would not

contribute to the zero sequence voltages (ex: 1-5', 2-4' etc.). For these combinations  $SW_1$  through  $SW_4$  may be closed without resulting in zero sequence currents. Other combinations that may be used are the ones with a zero switching state for one inverter at one end of the load phase, (ex: 7-4', 5-8' etc.). When one of the inverters is clamped to a zero state, the auxiliary switches connecting that inverter to the DC bus are opened creating an isolated switched neutral. Under these conditions the zero sequence currents would not flow for the lack of a return path. The space phasor combinations and the voltage space phasor positions used in this work are shown (solid lines) in Fig.4. The 64 voltage space phasor locations form the vertices of 24 equilateral triangles, which are referred to as 24 sectors (Fig.3). Six adjacent sectors together form a hexagon. Six such hexagons can be identified with their centers located at **A**, **B**, **C**, **D**, **E** and **F** respectively (Fig.3). In addition there is one inner hexagon with its center at **O**. For the present work the triangular sectors used for generating PWM switching are shown in Fig.4. The equilateral triangles numbered '1' through '6' are referred to as 'inner sectors', the equilateral triangles numbered '7' through '12' are referred to as 'middle sectors' and the obtuse angled isosceles triangles numbered '13' through '18' are referred to as 'outer sectors' (Fig. 4). To implement the PWM pattern, the triangular sector in which the tip of the reference space phasor lies is first identified and sub-hexagon to which it belongs is found out using Fig.6. The sector identification is based on level comparators along  $ja$ ,  $jb$ ,  $jc$  axes perpendicular to the  $a$ ,  $b$ ,  $c$  axes respectively (Fig.6)[7]. The sector is identified by computing and comparing components of the reference voltage phasor along  $ja$ ,  $jb$ , and  $jc$  axes with fixed levels, as shown in Fig.6[7]. The Components of the reference space phasor along the  $ja$ ,  $jb$ ,  $jc$  axes defines the sector boundaries and can be used for detecting the sectors[7]. The PWM strategy adopted is based on whether the tip of the reference voltage space phasor lies in the inner sectors (sectors '1' through '6'), or in the middle sectors (sectors '7' through '12') or in the outer sectors (sectors '13' through '18') (Fig.4). In the following sections the PWM strategies adopted for the above three cases are explained.

#### IV. Space-phasorbased PWM switching strategy for inner sectors:

If the tip of the reference voltage space-phasor lies in the inner hexagon with center at **O** (Fig.4), a space phasor based scheme as suggested in reference [4] has been adopted. In this scheme, a space phasor based PWM strategy is proposed based on the instantaneous values of the reference voltages of  $a$ ,  $b$ ,  $c$  phases [4]. This method does not depend on the magnitude of the reference voltage space phasor and its relative angle with respect to the reference axis ( $\alpha$  - axis placed along 'a' phase axis).

This method is extended for the dual inverter scheme ( for PWM pattern generation in inner sectors '1' through '6') by clamping an inverter at one end of the load phase while the inverter at the other end is switched. This switching strategy also ensures that each inverter is switched for ' $n/2$ ' times with half the DC- link voltage when compared to a conventional single inverter scheme switching for ' $n$ ' times in one cycle of the load phase voltage. The actual switching times for each inverter leg is obtained in the same way as that of the single inverter scheme [4]. Each cycle of the load phase voltage is divided into 48 equal sub-intervals as shown in Fig.7. Each of this sub-interval duration corresponds to the sampling interval,  $T_s$ . This division is maintained for the entire modulation range with V/f control.

#### V. Space-phasorbased PWM switching strategy for outer sectors

The outer sectors are isosceles triangles (not equilateral triangles as in the case of the inner sectors '1' through '6') because the inverter switching vector locations **G**, **I**, **K**, **M**, **P**, **R** (Fig.4) are not used for the present work, as these switching vectors introduce triplen harmonics, which are suppressible only by the use of harmonic filters or isolation transformers). In Fig.8, the reference voltage vectors **OV<sub>1</sub>** and **OV<sub>2</sub>** at two different time instants are shown with their tips lying in sectors 13 and 11 respectively. In sector-13 the vector **OV<sub>1</sub>** can be generated using vector **OA** and **AV<sub>1</sub>**. The vector **AV<sub>1</sub>** is not directly available from the space phasor combinations (Fig.4) and hence is to be generated from the adjacent active switching vector locations using volt-sec balance. In sector-13 the vector **AV<sub>1</sub>** can be realized by switching between the vectors **OA**, **OH** and **OS** for periods  $T_0$ ,  $T_1$  and  $T_2$  respectively, in a sampling period  $T_s$ . The periods  $T_0$ ,  $T_1$  and  $T_2$  for vector **AV<sub>1</sub>** in sector-13 can be found out by mapping the vector **AV<sub>1</sub>** to **OV<sub>1</sub>** by shifting the point 'A' to 'O'. By shifting the point 'A' to 'O', the outer isosceles triangle **ASH** is mapped to an inner isosceles triangle **OFB** (Fig.8). Adopting the same procedure, the rest of the outer sectors (14 to 18) may also be mapped into the corresponding inner isosceles triangles. The expressions for the active vector switching time periods  $T_1$  and  $T_2$  in terms of the instantaneous reference phase voltages are not presented here for brevity. The switching periods can be easily calculated from the instantaneous reference phase voltages (Table-2).

#### VI. Space-phasorbased PWM switching strategy for middle sectors

The switching timings  $T_0$ ,  $T_1$  and  $T_2$  for the inner sectors '7' through '12' can easily be determined from that of the procedure followed for the inner sectors [4][7]. From Fig.3, it

may be noted that the space phasor combinations from the dual inverter scheme produce a total of 24 triangular sectors. These sectors can be grouped into 7 sub-hexagonal groups with centers at **A**, **B**, **C**, **D**, **E**, **F** and **O** respectively. By mapping the centers of the sub-hexagons 'A' through 'F' to the point 'O' the middle sectors '7' through '12' get mapped to a corresponding inner sector ('1' through '6'). Once the appropriate inner sector is identified, The inverter vector switching periods  $T_0$ ,  $T_1$  and  $T_2$  are determined corresponding to the inner sector and the inverter vectors forming the middle sectors are chosen for the **PWM** switching [7].

## VII. Experimental Results

The proposed scheme is implemented for a 1 H.P., 3-phase induction motor drive in open loop with V/f control for different reference voltages covering the entire speed range. Fig.9 (a) shows the pole voltages of the individual inverters ( $v_{ao}$  and  $v_{a'o}$ ) and the motor phase voltage  $v_{aa'}$  (middle trace) containing triplen harmonic content for reference space phasor voltage  $|v_{sr}| = 0.4V_{dc}$  (in this case the tip of the reference voltage space phasor is confined to the inner sectors for the entire cycle in this case). Fig.9 (b) shows the motor phase voltages without the triplen harmonic content and the motor current at no-load for  $|v_{sr}| = 0.4V_{dc}$ . Fig.9(c) shows the harmonic spectra for the motor phase voltage and the motor phase voltage after the elimination of the triplen harmonics for  $|v_{sr}| = 0.4V_{dc}$ . Fig.10 (a) shows the pole voltages of the

individual inverters ( $v_{ao}$  and  $v_{a'o}$ ) and the motor phase voltage  $v_{aa'}$  (middle trace) containing triplen harmonic content for reference space phasor voltage  $|v_{sr}| = 0.6V_{dc}$  (in this case the tip of the reference voltage space phasor is confined to the middle sectors for a part of the cycle and to the outer sectors for the rest of the cycle). Fig.10 (b) shows the motor phase voltage without the triplen harmonic content and the motor current at no-load for  $|v_{sr}| = 0.6V_{dc}$ . Fig.10(c) shows the harmonic spectra for the motor phase voltage and the motor phase voltage after the elimination of the triplen harmonics for  $|v_{sr}| = 0.6V_{dc}$ . Fig.11 (a) shows the pole voltages of the individual inverters and the motor phase voltage  $v_{aa'}$  for  $|v_{sr}| = 0.9V_{dc}$ . In this case, the tip of the reference voltage space phasor is forced to trace the hexagon HJLNQS (fig.4) and corresponds to the case of over-modulation as  $|v_{sr}| > 0.75V_{dc}$ . During over-modulation the inverter voltage vector positions at locations **H**, **J**, **L**, **N**, **Q** and **S** are used (Fig.4). It may be noted that the space-vector combinations corresponding to these positions will not contribute to triplen harmonics (Table-1). Fig.11@ shows the motor phase voltage and the motor current at no-load for  $|v_{sr}| = 0.9V_{dc}$ . Fig.11 (c) shows the harmonic spectrum of the motor phase voltage, for  $|v_{sr}| = 0.9V_{dc}$ . It may be observed that  $v_{aa'}$  does not contain any triplen harmonic content in this case as explained above. In all these experiments the triplen harmonics are eliminated by realizing switched neutrals using the auxiliary switches (sw1-sw4, Fig.5).

Table-1: Third harmonic contributions from the space-phasor combinations

$-V_{dc}/2$	$-V_{dc}/3$	$-V_{dc}/6$	0	$V_{dc}/6$	$V_{dc}/3$	$V_{dc}/2$
8-7'	8-4'	8-5' 8-3'	8-8' 5-5' 5-3'	5-8' 3-8'	4-8'	7-8'
	8-6'	5-4' 3-4'	3-5' 3-3' 4-4'	4-5' 4-3'	6-8'	
	8-2'	8-1' 5-6'	5-1' 3-1' 4-6'	4-1' 1-8'	2-8'	
	5-7'	5-2' 3-6'	4-2' 1-5' 1-3'	6-5' 6-3'	7-5'	
	3-7'	3-2' 4-7'	6-4' 2-4' 1-1'	2-5' 2-3'	7-3'	
	1-7'	1-4' 1-6'	6-6' 6-2' 2-6'	7-4' 6-1'	7-1'	
		1-2' 6-7'	2-2' 7-7'	2-1' 7-6'		
		2-7'		7-2'		

Table-2: The expressions for the active vector switching times  $T_1$  and  $T_2$  in the outer sectors

Sector before transformation	Sector after transformation	Clamped Phase	Sector number	$T_1$	$T_2$
ASH	OFB	A	13	$(2T_s/V_{dc})(v_a-v_b)$	$(2T_s/V_{dc})(v_a-v_c)$
BHJ	OAC	C	14	$(2T_s/V_{dc})(v_a-v_c)$	$(2T_s/V_{dc})(v_b-v_c)$
CJL	OBD	B	15	$(2T_s/V_{dc})(v_b-v_c)$	$(2T_s/V_{dc})(v_b-v_a)$
DLN	OCE	A	16	$(2T_s/V_{dc})(v_b-v_a)$	$(2T_s/V_{dc})(v_c-v_a)$
ENQ	ODF	C	17	$(2T_s/V_{dc})(v_c-v_a)$	$(2T_s/V_{dc})(v_c-v_b)$
FQS	OEA	B	18	$(2T_s/V_{dc})(v_c-v_b)$	$(2T_s/V_{dc})(v_a-v_b)$

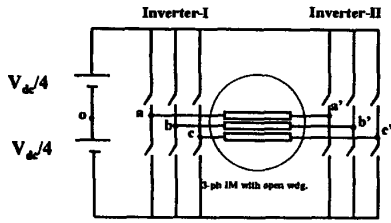


Fig.1 Dual inverter fed induction motor with open end winding

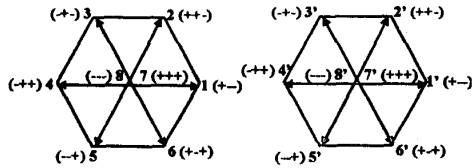


Fig.2 Space phasor locations for Inverter-I (Left) and Inverter-II (Right)

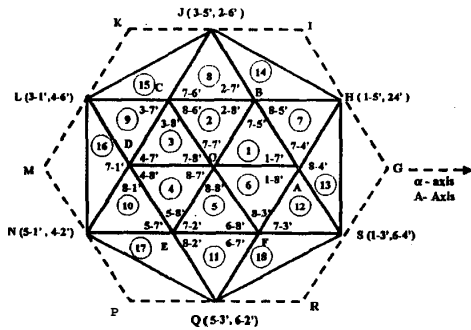


Fig.4 Space phasor combinations used for the proposed dual-inverter scheme

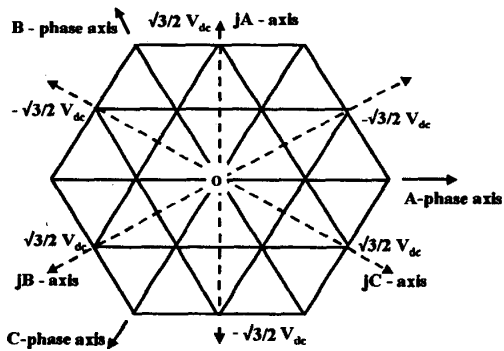


Fig.6 Sector identification using ja, jb and jc axes

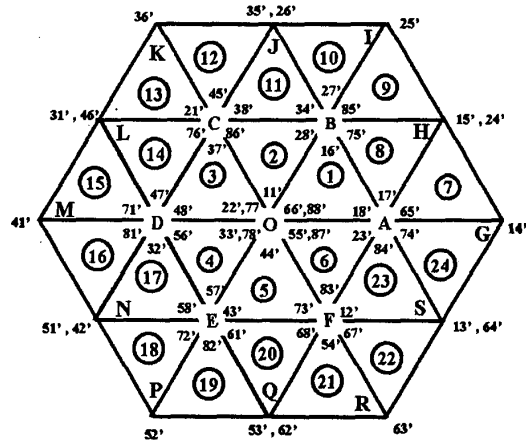


Fig.3 Voltage space phasor combinations from the dual-inverter scheme

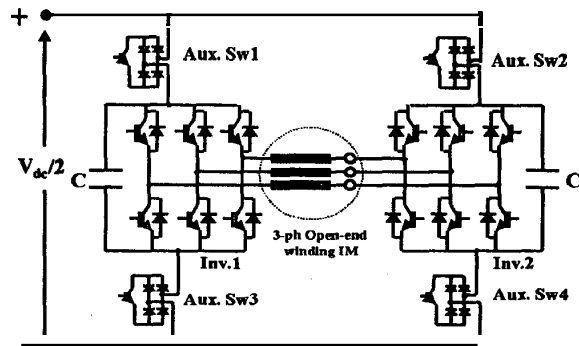


Fig.5. Proposed power circuit schematic

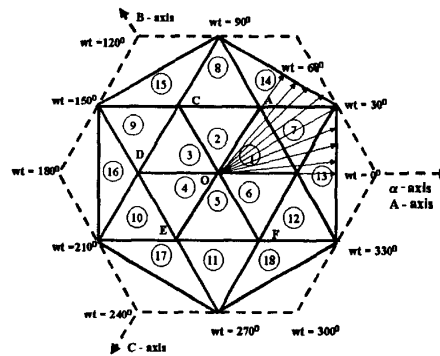


Fig.7 Illustration of 48-sampling intervals for one cycle of operation

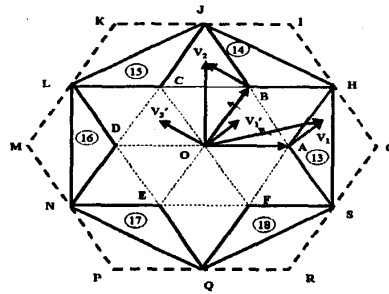


Fig.8 Resolution of the reference voltage space phasors

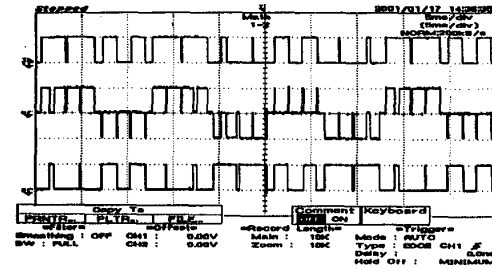


Fig.9a. Pole voltages of individual Inverters and phase voltage with triplen harmonic content (middle trace) for  $|V_w| = 0.4V_{dc}$

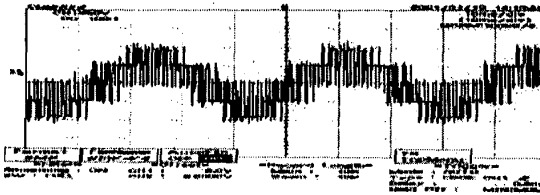


Fig.9b. The motor phase voltage (50V/div) without the triplen harmonic content and phase current (1Amp/div) for  $|V_w| = 0.4V_{dc}$

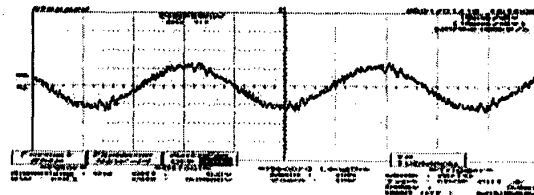


Fig.9c. Normalized harmonic spectrum of the phase voltage without (Left) and with (Right) the suppression of the triplen harmonic content for  $|V_w| = 0.4V_{dc}$  (Experimental result)

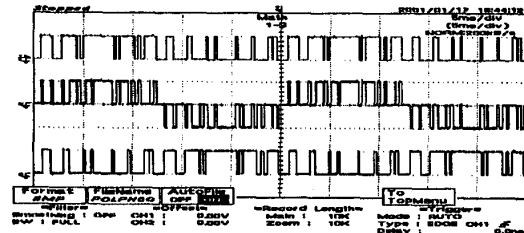


Fig.10a. Pole voltages of individual Inverters and phase voltage with triplen harmonic content (middle trace) for  $|V_w| = 0.6V_{dc}$

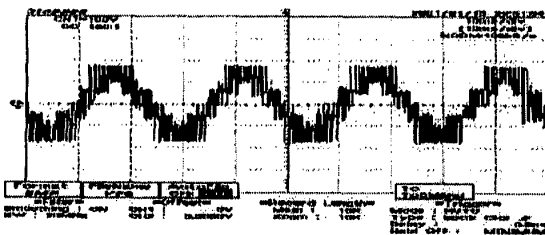


Fig.10b. The motor phase voltage (100V/div) without the triplen harmonic content and phase current (1Amp/div) for  $|V_w| = 0.6V_{dc}$

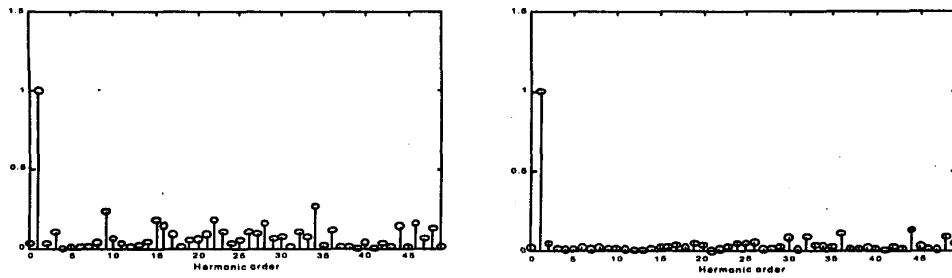


Fig.10c. Normalized harmonic spectrum of the phase voltage without (Left) and with (Right) the suppression of the triplen harmonic content for  $|V_{sr}| = 0.6 V_{dc}$  (Experimental result)

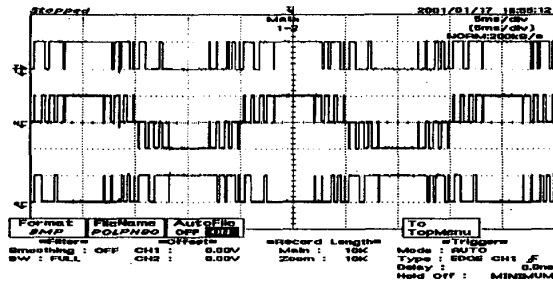


Fig.11a. Pole voltages of individual inverters and phase voltage without triplen harmonic content (middle trace) for  $|V_{sr}| = 0.9 V_{dc}$

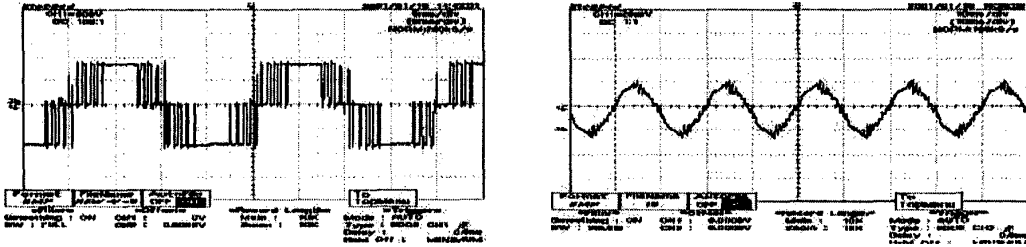
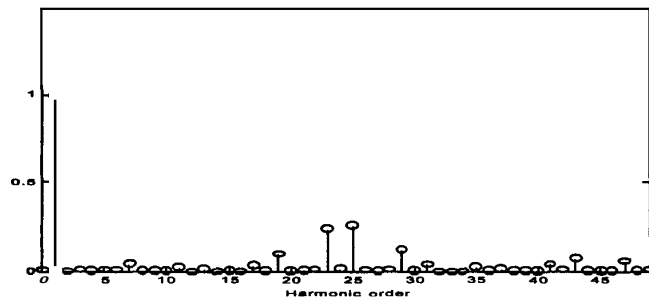


Fig 11b. The motor phase voltage (200V/div) without the triplen harmonic content and phase current (1Amp/div) for  $|V_{sr}| = 0.9 V_{dc}$



Normalized harmonic spectrum of the phase voltage for  $|V_{sr}| = 0.9 V_{dc}$  (The triplen harmonic content in the phase voltage is zero in this case). (Experimental result)

## VIII. Conclusion

- A novel dual two-level inverter fed open-end winding induction motor drive has been proposed in this paper. The proposed scheme produces voltage space phasor locations similar to that of a 3-level inverter.
- A novel **PWM** switching strategy aimed to suppress the zero sequence currents is also proposed in this paper, eliminating the need for bulky harmonic filters or isolation transformers.
- Each inverter is working with about half the DC link voltage when compared to a conventional 2-level inverter drive.
- The each inverter switching frequency is half to that of the motor phase switching frequency.
- Split level voltage fluctuations are absent in the proposed scheme, when compared to a 3-level inverter.

## IX References

- [1] A.Nabae, I.Takahashi, and H.Agaki, "A new neutral-pointslamped PWM inverter". *IEEE Trans.Ind.Appl.* vol.1A-17, pp518-523, Sept/ Oct 1981.
- [2] P.M.Bhagwat and V.R.Stefanovic, "GeneralizedStructure of a multi level PWM inverter", *IEEE Trans.Ind.Appl.* vol.1A-19, pp. 1057-1069, Nov./Dec.1983.
- [3] H.Stemmler, P.Guggenbach, "Configurationsof high power voltage source inverter drives", EPE conference 1993, pp. 7 - 12.
- [4] Joohn-Sheok Kim, Seung-Ki Sul," A Novel Voltage Modulation Technique of the Space Vector P W M IPEC-1995, pp. 742 - 747.
- [5] Bakari Mwinyiwiwa, Zbigniew Wolanski. "Multi-~~modular~~ Multilevel Converters with input/output Linearity",*IEEETrans.Ind.Appl.*, vol.33,No.5, Sept./Oct 1997,pp 1214-1219.
- [6] A.Rufer, M.Veenstra, K.Gopakumar, "Asymmetric multilevel converter for high resolution voltage phasor generation", *EPE'99-Lausanne*, pp. PI-PIO.
- [7] E.G.Shivakumar, K.Gopakumar, S.K.Sinha, and Andre Pittet, V.T.Ranganathan, " Space vector PWM control of **dual** inverter **fed** open-end winding inductin motor drive", *IEEE-APEC-2001*, pp. 394-404.